EUROPEAN ORGANIZATION FOR NUCLEAR RESEARCH

CERN-EP/81-71
16 July 1981

ANGULAR DISTRIBUTIONS IN THE DIMUON HADRONIC PRODUCTION AT 150 GeV/c

NA3 COLLABORATION

J. Badier[4], J. Boucrot[5], J. Bourotte[4], G. Burgun[1], O. Callot[5], Ph. Charpentier[1], M. Crozon[3], D. Decamp[5], P. Delpierre[3], P. Espigat[3], B. Gandois[1], R. Hagelberg[2], M. Hansroul[2], Y. Karyotakis[5], W. Kienzle[2], P. Le Dû[1], J. Lefrançois[5], Th. Leray[3], J. Maillard[3], A. Michelini[2], Ph. Miné[4], G. Rahal[1], O. Runolfsson[2], P. Siegrist[1], A. Tilquin[3], J. Valentin[3], R. Vanderhaghen[4], S. Weisz[4].

CEN, Saclay[1]-CERN, Geneva[2]-Collège de France, Paris[3]-
Ecole Polytechnique, Palaiseau[4]-Laboratoire de l'Accélérateur Linéaire, Orsay[5].

ABSTRACT

From π^- interactions at 150 GeV/c on a heavy target, we present the final analysis of dimuon decay angle in the mass interval 4.5 to 8.5 GeV/c^2. Results are presented and discussed in various reference frames and are also given in terms of the density matrix elements. Finally the possibility of higher-twist effects at large x_1 is discussed; we find that our data are not compatible with Berger's model for these effects.

Submitted to Zeitschrift für Physik C

This paper describes the angular distribution of dimuons measured by the NA3 experiment using π^- at 150 GeV on a platinum target. The large number of available events and the wide spectrometer acceptance allow us to analyse our data in the θ,ϕ plane. In section 1, we discuss some technical points : data selection, acceptance, method of analysis. Section 2 presents the experimental results , and section 3 presents a discussion of these results. Section 4 is devoted to a test of higher twist effects.

1. TECHNICAL POINTS

General description of the apparatus, trigger and reconstruction procedure has already been published [1]. In the following we describe some specific points relevant to the data analysis. Let us recall that about 12 10^6 triggers were collected using a 150 GeV/c π^- beam traversing two targets in front of the beam absorber; in the next sections we speak only of events coming from the 6 cm platinum target centered at 40 cm from the upstream face of the beam dump. Due to poor statistics we do not consider here the events coming from the 30 cm hydrogen target centered at 60 cm from the platinum target.

a) Definition of the angles :

In the dimuon rest frame, we use 3 vectors (Fig.1) : the π one along the incoming π^- direction : $(\vec{\pi})$,the nucleon one $(\vec{N})$, and the μ^- one $(\vec{\mu})$. The reaction plane is the plane containing $\vec{\pi}$ and $\vec{N}$. An axis $\vec{L}$ is defined in this plane, the choice being somewhat arbitrary. We have used three alternative definitions of $\vec{L}$, as proposed by the litterature : $\vec{L} = \vec{\pi}$ (Gottfried-Jackson frame, "GJ"), $\vec{L} = -\vec{N}$ (u channel axis, "u"), and $\vec{L}$ as the bisector of $\vec{\pi}$ and $-\vec{N}$ (Collins-Soper frame, "CS"). The angle θ is defined as $\theta = (\vec{\mu}, \vec{L})$. Then, let ϕ be the angle between the reaction plane (containing $\vec{\pi}$ and $\vec{N}$) and the $(\vec{\mu}, \vec{L})$ plane, positive in the $\vec{\pi} \times \vec{N}$ hemisphere.

It is worthwile to comment on the choice of the $\vec{L}$ axis. In the framework of the Drell-Yan model, the muon pair is assumed to be produced by $q\bar{q}$ annihilation. In this case, the "good" axis is the $q\bar{q}$ line of flight. But this axis is unknown, and we must make some hypothesis in order to connect $\vec{\pi}$ and $\vec{N}$ with $q\bar{q}$ axis. This is related to the transverse momentum of the dimuon, which is assumed to be due to the nucleon (GJ), the pion (u) or equally shared (CS). The angles between GJ and CS, and between CS and u are of the order P_t/M, P_t being the transverse momentum and M the mass of the dimuon.

b) Selection of the events

In the present analysis we are interested by events produced in the so-called "continuum" region on the platinum target. A first cut is performed on the dimuon mass , to eliminate resonances (J/ψ and T). A second cut is performed on the Feynman variable X_F of the dimuon to eliminate events produced by secondary interactions in the platinum target. Using reasonable models, one can estimate that these background events represent only a few percent at positive X_F, but their fraction increases quickly at negative x_F. We then eliminate all events at negative X_F. Another problem comes from J/ψ particles produced at the hydrogen target and wrongly assigned to the platinum target, so that their mass is found to be larger then 4 GeV/c^2. A Monte-Carlo simulation shows that these events represent a small fraction ($\sim$1%) of true platinum events, essentially in the mass range 3.8 to 4.5 GeV/c^2, and however they have an abnormal angular distribution. We choose then to cut these events by requiring the mass of the dimuon to be between 4.5 and 8.5 GeV/c^2. Having applied all these cuts we are left with about 15 000 events

The last source of background is originated by muons coming from π and K decays. It can be estimated using like sign muon pairs, which are less than 1% of the opposite sign events, but are concentrated at large $|\cos\theta|(> 0.8)$ where they represent about 20% of the events. We subtract then these events bin per bin, to eliminate opposite sign pairs coming from hadron decays.

c) Monte Carlo

Simulation of the experiment is performed using Monte Carlo technique. We generate dimuons using the Drell-Yan model with structure functions from deep inelastic scattering (CDHS experiment [2]) for the nucleon and from our results from the pion [3]. Transverse momentum is generated according to a phenomenological parametrization of our data [3], and uncorrelated with any other variable.

Assuming a spin 1 for the dimuon (virtual photon) and parity conservation, the differential cross section can be written as :

$$\frac{1}{\sigma}\frac{d^2\sigma}{d\cos\theta\, d\phi} = \frac{3}{4(A+2)}\left(1 + \cos^2\theta + A\sin^2\theta + B\sin 2\theta\cos\phi + C\sin^2\theta\cos 2\phi\right) \qquad (1)$$

We want to measure A, B and C in various intervals of M, P_T, x_1. This is done by a global fit of the θ, ϕ distribution,as described later, but we can already remark that each coefficient is mainly determined by the distribution in a specific region : A is related to the $\cos\theta$ distribution integrated over ϕ, B by the ϕ distribution for large values of $\sin 2\theta$ (i.e. $|\theta| = \pi/4 \pm \pi/8$) and C by the ϕ distribution for $\sin^2\theta \sim 1$ (i.e. $|\theta| = \pi/2 \pm \pi/8$).As an illustration, we show on fig.2 the acceptance in these regions. We can see on this figure that the acceptance decreases strongly at large $\cos\theta$, and thus that A is very sensitive to systematic effects arising at large $\cos\theta$ values; the cuts on the sample of events described before have been made in order to obtain a cleaner sample in this region. For B and C, the situation is better, and systematic effects are then small.

d) Technical method

Having defined the kinematical region for the present analysis, we obtain the corresponding sample of events in the $\cos\theta$, ϕ plane. Using our Monte Carlo program, we generate events with a certain value of A, B and C. We thus obtain a two dimensional distribution in the $\cos\theta$, ϕ plane of these reconstructed "pseudo-events". Eq.(1) shows that this distribution is a linear combination of four distributions, with relative weights A, B and C. We adjust then A, B and C to reproduce the experimental data.

The main advantage of this global method is to determine A, B and C with the corresponding acceptance, and to measure correlations between these terms. We have tried other methods, and different choices of the bin sizes to be sure that the values of A, B, C do not depend strongly on a particular technique. The Monte Carlo program has been carefully checked, and reproduces quite well all impact distributions of particles in the detectors, including all known inefficiencies. We are then confident that systematic effects are smaller than the statistical error.

2) RESULTS

As mentioned before, we have analysed dimuons produced by 150 GeV pions on a platinum target. The mass interval is 4.5 to 8.5 GeV, the Feynman X_F is positive and we subtract the like sign dimuon pairs. We determine the A, B and C coefficients defined in Eq.(1), and present the results as λ, B and C, λ being the standard parameter $d\sigma/d\cos\theta \propto 1 + \lambda\cos^2\theta$, which is equal to $(1 - A)/(1 + A)$. First we look at values of λ, B and C in the Collins Soper frame.

1a) Mass dependence

Table 1 gives the values obtained in 3 mass bins. No significant variation is observed and for the following analysis we integrate over the selected mass interval.

1b) x_1 dependence

Table 2 gives the values obtained as function of x_1, for small and large values of P_T. Here also, we don't see significant variations with x_1. Higher twist effects are expected to appear at x_1 near 1, and this point will be discussed in detail in section 4.

1c) P_T/M dependence

We choose this dimensionless variable instead of P_T, because this is the most commonly used by theoretical calculations, and because this is also a measurement of the angle between the various reference frames.

Fig.3 and table 3 give results in the CS frame. A clear variation of B and C is observed. As usual, we parametrize B and C with linear and quadratic dependence with P_T/M. Values are the following

$$B = (-0.6 \pm 0.2)\ P_T/M$$
$$C = (\ 1.5 \pm 0.5)\ (P_T/M)^2$$

The negative sign of B is directly related to our particular definition of the ϕ angle origin and sign. Due to the large error bars, the parametrization of λ is not very significant and is compatible with the standard assumption A = 2C [5]

2) Gottfried-Jackson frame

The variations of λ, B and C as a function of P_T/M are given in fig.4 and table 4. The B and C parameters vary faster than in the Collins-Soper frame and may be parametrized as follows :

$$B = -(1.4 \pm 0.2)\ P_T/M$$
$$C = (2.0 \pm 0.5)\ (P_T/M)^2$$

In this frame λ is almost independent of P_T/M ($\lambda \sim 0.6$) but is as badly measured as in the Collins-Soper frame.

In fig.5 are displayed the variations of λ, B and C as a function of x_1. No significant variation is found for λ at high x_1 values.

3) u frame

In this frame the B coefficient is found compatible with 0 (fig.6), which implies that the angular distribution reduces to the simple form

$$1 + \lambda\cos^2\theta + C\ \sin^2\theta\ \cos^2\phi \text{ with } C \sim 1.4\ P_T^2/M^2$$

An even better adjustment is found with $C = 0.6\ P_T/M$.

The relation $A = 2C$ is satisfactorily verified; no significant variation of λ, B and C is found as a function of x_1.

4) Comparison with various predictions

As we have seen, the relation $A = 2C$ is verified by our data, although A is poorly determined. This relation is very general and holds for spin 1/2 interacting partons; it has been shown [5] that it has no first order QCD corrections.

The variation of A, B and C with P_T/M has been predicted by Collins [6] from first order QCD corrections (the transverse momentum being balanced through the emission of a gluon). The predictions are : $B \sim P_T/M$ and $C = 1/2\ P_T^2/M^2$ in the Collins-Soper frame. As we have seen above, we find that these relations are qualitatively satisfied but C is found experimentally 3 times larger than predicted. However it should be noticed that the model does not take into account the quark primordial transverse momentum, which is expected to be substantially contributing up to the highest values of P_T/M experimentally available.

An attempt has been done [7] to test the spin of the gluon with high transverse momentum data ($P_T > 2$ GeV/c), in the framework of hard gluon emission with large P_T. Our data at these transverse momentum are quite poor and do not allow a quantitative prediction (last point on fig.4c).It can just be said that they are more compatible with the value expected from a vector gluon.

3) DENSITY MATRIX FORMULATION

Assuming a spin 1 for the virtual photon decaying into $\mu^+\mu^-$, it is possible to express the density matrix elements in terms of the A, B and C parameters defined in Eq.(1)

$$\rho_{00} = \frac{A}{A+2}\ ,\ \mathrm{Re}\ \rho_{10} = -\frac{B}{\sqrt{2}(A+2)}\ ,\ \rho_{1-1} = \frac{C}{A+2} \qquad (2)$$

If we use the A, B and C parameters found in the u-channel frame, it is possible to apply the rotation operator to the density matrix in order to find the elements in a new frame rotated by an angle β around the Oy axis :

$$\begin{aligned}
\rho_{00}(\beta) &= \rho_{00} + X \sin^2\beta + 2\sqrt{2}\ \mathrm{Re}\ \rho_{10} \sin\beta \cos\beta \\
\rho_{1-1}(\beta) &= \rho_{1-1} + \frac{X}{2}\sin^2\beta + \sqrt{2}\ \mathrm{Re}\ \rho_{10} \sin\beta \cos\beta \\
\mathrm{Re}\ \rho_{10}(\beta) &= \frac{X}{\sqrt{2}} \sin\beta \cos\beta + \cos 2\beta\ \mathrm{Re}\ \rho_{10}
\end{aligned} \qquad (3)$$

where $X = \dfrac{1 - 3\rho_{00} - 2\rho_{1-1}}{2} = \dfrac{1 - A - C}{A + 2}$

A good parameter is the angle β_0, for which $\mathrm{Re}\ \rho_{10}(\beta_0)$ vanishes :

$$\mathrm{tg}\ 2\beta_0 = -\frac{2\sqrt{2}\ \mathrm{Re}\ \rho_{10}}{X} = \frac{2B}{1 - A - C}$$

In the same way the most significant parameters to describe the decay are :

$$R_{0\,0} = \rho_{0\,0}(\beta_0) = \frac{A - B(1 - \cos 2\beta_0)/\sin 2\beta_0}{A + 2} \qquad (4)$$

$$R_{1\,-1} = \rho_{1\,-1}(\beta_0) = \frac{C - B(1 - \cos 2\beta_0)/2\sin 2\beta_0}{A + 2}$$

The positivity of the matrix is expressed by the conditions :

$$0 < R_{0\,0} < 1 - 2\,|R_{1\,-1}| \qquad (5)$$

For a set of events having a same value of $\alpha = 2P_t/M$, the A, B and C coefficients in the Gottfried-Jackson and the Collins Soper frames can be calculated from those estimated in the u-channel frame.

The results are displayed in table 6 and Fig.7 and 8; one can remark that β_0 corresponds to the minimum value of $R_{0\,0}$ and $R_{1\,-1}$.

Assuming a linear variation for β_0, and a quadratic variation for $R_{1\,0}$ and $R_{1\,-1}$ with P_t/M, one obtains from our sample of events

$$\beta_0 = (0.27 \pm 0.16)\,\frac{P_t}{M}$$

$$R_{0\,0} = (0.9 \pm 0.6)\,\left(\frac{P_t}{M}\right)^2$$

$$R_{1\,-1} = (0.72 \pm 0.2)\,\left(\frac{P_t}{M}\right)^2$$

β_0 is smaller than P_t/M and $R_{1\,-1}$ is significantly different from 0. $R_{0\,0}$ is compatible with the generally accepted hypothesis $R_{0\,0} = 2R_{1\,-1}$. Imposing this constraint, we get $R_{1\,-1} = (0.6 \pm 0.2)(P_t/M)^2$. Furthermore, one has to remark that $R_{0\,0}$ is also compatible with 0.

These results can be interpreted in a naive model. Assuming massless and unpolarized quarks, the density matrix of a dimuon produced in an $q\bar{q}$ annihilation, measured with respect to the quark line of flight is :

$$\begin{pmatrix} 1 & 0 & 0 \\ 0 & 0 & 0 \\ 0 & 0 & 1 \end{pmatrix}$$

The angle of these quark lines of flight with the u-channel axis is distributed according to a law $W(\beta)$. The final density matrix is such that :

$$< \beta > = \beta_0$$

$$\text{Var } (\beta) = 4R_{1-1} = 2R_{00}$$

In such a model,our results suggest that the $q\bar{q}$ line of flight is centered near the nucleon's one, with a large spread. This means that the contribution to the transverse momentum coming from the pion is greater than from the nucleon. As already seen, there is no striking dependence of the decay distribution with x_1 (fig.5).

It should ne noticed that the numerical values of A, B, C and λ given in tables 3 to 5 for the different frames, should be deduced exactly one from the other using table 6 and Eq.(3). This is not the case, due to some loss of information coming from the statistical method used to compute these coefficients from our finite sample of events.

4) HIGHER TWIST

1) Introduction

For $x_1 \to 1$ the angular distributions discussed above may be substantially modified by the so-called "higher twist effect". This effect - which is expected to be important only for incoming pions - comes from gluon exchange between an interacting quark from the pion or the nucleon, and the spectator valence quark in the pion (as can be seen in fig.9). Using specific assumptions, E. Berger [8] has computed the following expression for the cross section :

$$d\sigma \propto (1 - x_1)^2 (1 + \cos^2\theta) + \frac{4}{9}\frac{P_T^2}{M^2}\sin^2\theta + \frac{2}{3}\frac{P_T}{M}(1 - x_1)\sin 2\theta \cos\phi \qquad (6)$$

which is expected to be true only at large $x_1 (x_1 \to 1)$ in the Gottfried-Jackson frame.

Eq.(6) contains several interesting points. First it predicts that for $x_1 \to 1$ the virtual photon polarisation turns from transversal $(1 + \cos^2\theta)$ to longitudinal $(\sin^2\theta)$. Then, the pion structure function behaves as $(1 - x_1)^2$ when x_1 grows up to 1, and the cross section exhibits a large scale-breaking term proportional to $1/M^2$. No prediction for the $\sin^2\theta \cos 2\phi$ term, as expected from the general form of Eq.(1), is given in this model.

2) Experimental results

As Eq.(6) mixes five variables (x_1, P_T, M, θ, ϕ) it is quite difficult to check it extensively in the high x_1 region where statistics is rather limited.

As a function of x_1, our data are compatible with a $(1 - x_1)^2$ + constant distribution only for $x_1 > 0.7$. As we have only 2900 events for $x_1 > 0.7$ it is not possible to fit directly the 5 variables dependence of Eq.(6) to the data. We have chosen to extract from the data the numerical value of one parameter, H, defined as follows :

$$\frac{d\sigma}{dx_1 d\cos\theta d\phi} = P + QH + RH^2$$

with $P = (1 - x_1)^2 (1 + \cos^2\theta)$

$$Q = \frac{P_T}{M}(1 - x_1)\sin 2\theta \cos\phi$$

$$R = \frac{P_T^2}{M^2}\sin^2\theta$$

From Eq.(6), this parameter H is predicted to be exactly H = 2/3 when $x_1 \to 1$. From our data, taking into account all errors, we find (see ref.[3] for technical points) :

$H = 0.40 \pm 0.10$ for $x_1 > 0.7$ (2900 events)
$H = 0.20 \pm 0.10$ for $x_1 > 0.85$ (770 events)

As can be seen, this result is not compatible with the predicted value, and the variation of H as a function of x_1 excludes that $H \to 2/3$ when $x_1 \to 1$.

The ratio of the terms QH and P, which is predicted from Eq.(6) to behave as $\delta \simeq H/1-x_1$, is found experimentally to be flat :
$\delta \sim -1.7$ for $x_1 > 0.7$ and $\delta \sim -1.5$ for $x_1 > 0.85$.
Thus we find that the $\cos\phi$ distribution has not any important x_1 variation. The $\sin^2\theta \cos 2\phi$ term (which is absent from Berger's formula) cannot disturb substantially these conclusions since its ϕ integral is very small.

As a function of θ, the check between data and Eq.(6) is not conclusive since the $\sin^2\theta$ term has a very small weight when integrated over P_T/M, and our acceptance is poor at high $|\cos\theta|$.

We conclude that our data do not show a higher twist contribution of the size predicted by Eq.(6) when $x_1 \to 1$. However higher twist effects may exist at a lower level in this kinematical region.

This result is in contradiction with a previous measurement from the C.I.P collaboration [9] which found a variation of λ as a function of x_1, compatible with Eq.(6).

5) CONCLUSION

From this analysis of high-mass dimuon angular distributions, we will conclude that it was absolutely necessary to analyse simultaneously the θ and ϕ angular distributions since these variables are coupled by the acceptance of the spectrometer. The A, B and C coefficients we have found are compatible with QCD predictions. The B coefficient cancels out in the u-channel frame, but is significantly different from zero in the Gottfried-Jackson frame. The C coefficient does not vary strongly from one frame to the other, and is significantly different from zero. The A coefficient has large errors; it is compatible with the theoretical relation $A = 2C$ but also compatible with zero.

Our data at large x_1 are not compatible with the particular description of higher twist effects given by E. Berger. The question of the existence of these effects remains open.

We are much indebted to the CERN SPS operating crew and the Experimental Area group, which provided us with a very powerful beam line. We would also thank all the technical staff of the NA3 collaboration for their contribution to the construction of the apparatus, and the computer staffs at CERN, Paris IN2P3 and Saclay for the efficient processing of our very large amount of data.

REFERENCES

[1] J. Badier et al., Nucl. Instr. and Meth. 175 (1980) 319-330

[2] J. de Groot et al., Phys. Lett. 82B (1979) 456

[3] O. Callot, Thesis (unpublished) Orsay Report No LAL 81/05, April 1981

[4] C.S. Lam and W.K. Tung. Phys. Rev. D18 (1978) 2447

[5] J.C. Collins, Phys. Rev. Lett. 42 (1979) 291
C.S. Lam and W.K. Tung, Phys. Lett 80B (1979) 228,
Phys. Rev. D21 (1980) 2712

[6] J.C. Collins and D.E. Soper, Phys. Rev. D16 (1977) 2218
J.C. Collins. Phys. Rev. Lett. 42 (1979) 291

[7] P.W. Johnson and W.K. Tung, Phys. Rev. Lett. 45 (1980) 1382

[8] E.L. Berger, Z. Phys. C4 (1980) 289

[9] K.J. Anderson et al., Phys. Rev. Lett. 43 (1979) 1219

Table 1

Collins Soper, Mass ($x_F > 0$, $x_1 < 0.8$)

M	A	B	C	λ
4.5 - 5	0.11 ± 0.10	-0.09 ± 0.06	0.11 ± 0.05	0.81 ± 0.16
5 - 6	0.24 ± 0.12	-0.13 ± 0.06	0.13 ± 0.06	0.61 ± 0.15
6 - 8.5	0.13 ± 0.16	-0.19 ± 0.08	0.17 ± 0.08	0.77 ± 0.26

Table 2

Collins Soper, x_1, P_T ($x_F > 0$)

x_1	P_T	A	B	C	λ
0.2 - 0.4	<1	0.41 ± 0.50	-0.10 ± 0.16	0.12 ± 0.13	0.42 ± 0.57
0.4 - 0.6	<1	0.01 ± 0.12	-0.09 ± 0.07	0.06 ± 0.07	0.98 ± 0.23
0.6 - 0.8	<1	0.12 ± 0.13	-0.04 ± 0.09	0.19 ± 0.12	0.79 ± 0.21
0.8 - 1	<1	-0.11 ± 0.16	-0.02 ± 0.16	0.22 ± 0.19	1.25 ± 0.42
0.2 - 0.4	>1	-0.03 ± 0.26	-0.14 ± 0.12	0.18 ± 0.09	1.04 ± 0.60
0.4 - 0.6	>1	0.09 ± 0.13	-0.20 ± 0.06	0.18 ± 0.06	0.84 ± 0.22
0.6 - 0.8	>1	0.19 ± 0.15	-0.19 ± 0.08	0.08 ± 0.08	0.69 ± 0.22
0.8 - 1	>1	0.07 ± 0.21	-0.34 ± 0.14	0.29 ± 0.14	0.87 ± 0.38

Table 3

λ, A, B, C Collins-Soper frame

P_T/M	A	B	C	λ
0,0 - 0,1	0,12 ± 0,14	-0,15 ± 0,11	0,28 ± 0,14	0,79 ± 0,22
0,1 - 0,2	0,12 ± 0,11	-0,05 ± 0,06	0,05 ± 0,05	0,79 ± 0,17
0,2 - 0,3	0,10 ± 0,12	-0,14 ± 0,07	0,10 ± 0,05	0,82 ± 0,20
0,3 - 0,4	0,56 ± 0,31	-0,27 ± 0,12	0,23 ± 0,11	0,29 ± 0,27
> 0,4	-0.04 ± 0,23	-0,26 ± 0,13	0,32 ± 0,10	1,08 ± 0,53

Table 4

A, λ, B, C function of P_T/M Gottfried-Jackson frame

P_T/M	A	B	C	λ
0 - 0.1	0.11 ± 0.15	-0.26 ± 0.10	0.26 ± 0.15	0.81 ± 0.25
0.1 - 0.2	0.23 ± 0.12	-0.16 ± 0.06	0.05 ± 0.06	0.62 ± 0.16
0.2 - 0.3	0.26 ± 0.14	-0.37 ± 0.08	0.18 ± 0.06	0.59 ± 0.18
0.3 - 0.4	0.28 ± 0.21	-0.48 ± 0.13	0.26 ± 0.09	0.57 ± 0.27
0.4 - 0.5	0 ± 0.22	-0.63 ± 0.14	0.36 ± 0.12	1.0 ± 0.46
0.5 - 0.6	0.72 ± 0.70	-0.73 ± 0.47	1.05 ± 0.42	0.16 ± 0.57

Table 5

λ, A, B, C function of P_T/M u-frame

P_T/M	A	B	C	λ
0 - 0.1	0.10 ± 0.14	-0.06 ± 0.10	-0.01 ± 0.13	0.82 ± 0.24
0.1 - 0.2	0.07 ± 0.10	0.07 ± 0.05	0.04 ± 0.05	0.87 ± 0.17
0.2 - 0.3	0.08 ± 0.12	0.01 ± 0.07	0.14 ± 0.05	0.85 ± 0.20
0.3 - 0.4	0.31 ± 0.24	-0.01 ± 0.12	0.20 ± 0.09	0.53 ± 0.28
0.4 - 0.5	-0.01 ± 0.26	0.25 ± 0.16	0.26 ± 0.13	1.02 ± 0.57

Table 6

u-channel

P_T/M	β_0	R_{00}	R_{1-1}
0.0 - 0.1	-0.07 ± 0.10	0.05 ± 0.06	-0.01 ± 0.08
0.1 - 0.2	+0.08 ± 0.05	0.03 ± 0.04	0.02 ± 0.03
0.2 - 0.3	+0.01 ± 0.07	0.04 ± 0.06	0.07 ± 0.03
0.3 - 0.4	-0.02 ± 0.12	0.13 ± 0.10	0.09 ± 0.04
0.4 - 0.5	+0.33 ± 0.16	-0.04 ± 1.2	0.11 ± 0.06

FIGURE CAPTIONS

Fig. 1 Definition of axes and angles for dimuon production.

Fig. 2 Acceptance of NA3 spectrometer.
a) as a function of ϕ for different values of θ
b) as a function of $\cos\theta$.

Fig. 3 λ, B and C parameters as a function of P_T/M in the Collins-Soper frame.

Fig. 4 λ, B and C parameters as a function of P_T/M in the Gottfried-Jackson frame.

Fig. 5 λ, B and C parameters as a function of x_1 in the Gottfried-Jackson frame. Full circles : $P_T < 1$ GeV/c. Open circles : $P_T > 1$ GeV/c.

Fig. 6 λ, B and C parameters as a function of P_T/M in the u-channel frame.

Fig. 7 Variation of the density matrix elements $R_{0\,0} - R_{1\,-1}$, $\mathrm{Re}(R_{1\,0})$ as a function of a rotation β around the Oy axis.

Fig. 8 Coefficients $R_{0\,0}$ and $R_{1\,-1}$ as a function of P_T/M in the u-channel frame.

Fig. 9 Higher twist diagrams.

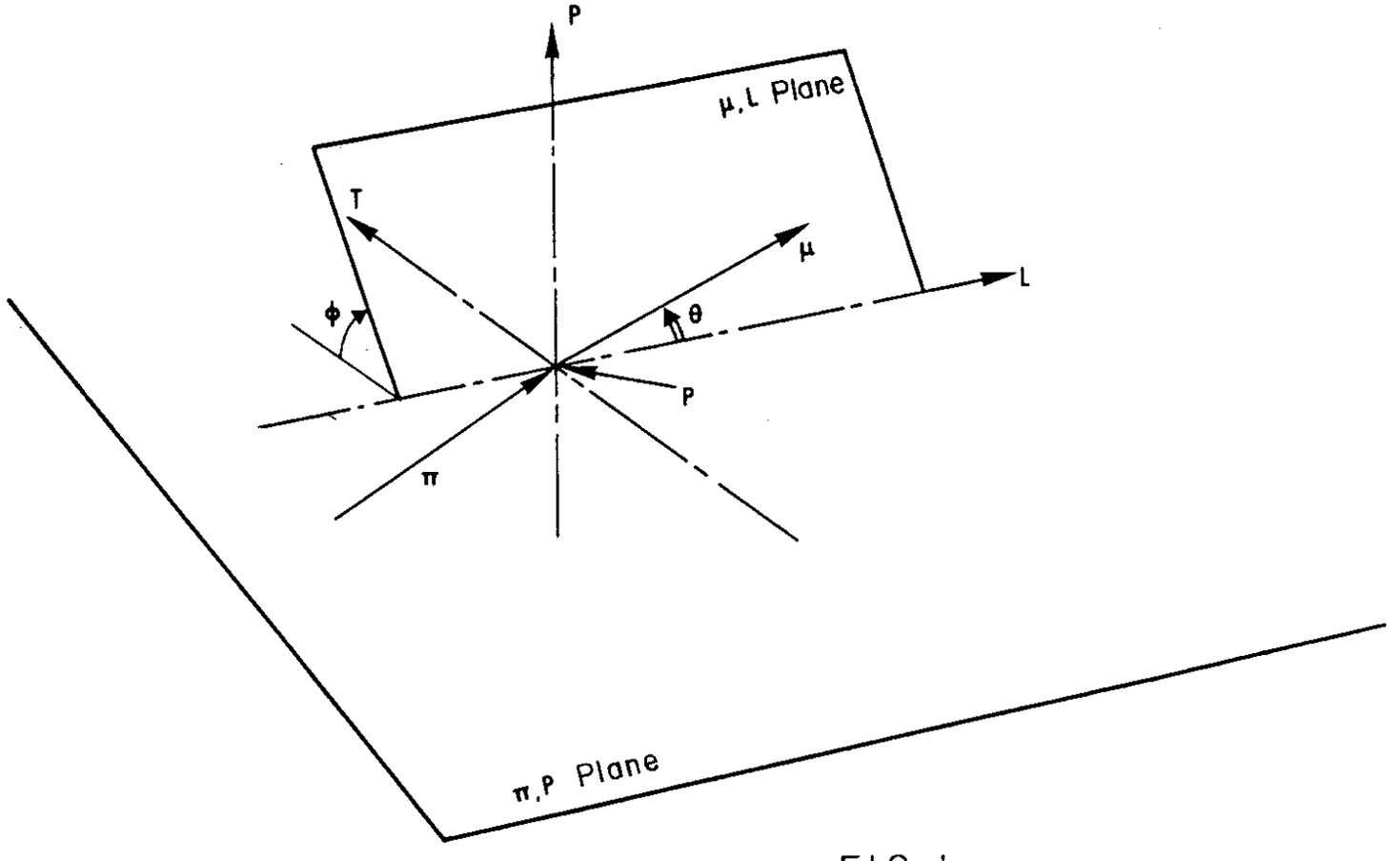

FIG. 1

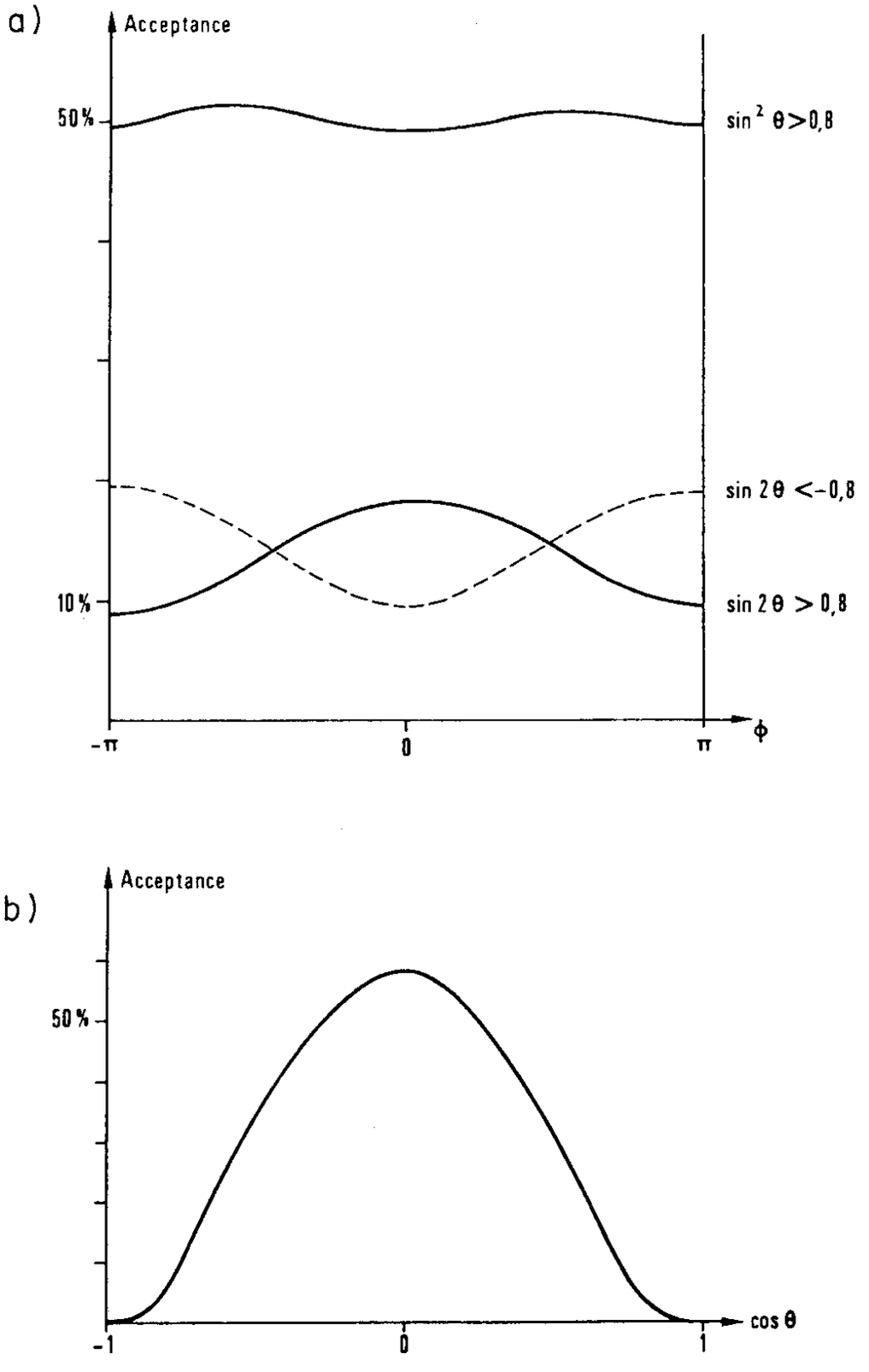
a)
Acceptance
50%
10%
sin² θ>0,8
sin 2θ <-0,8
sin 2θ > 0,8
-π
0
π
φ
b)
Acceptance
50%
-1
0
1
cos θ

FIG. 2

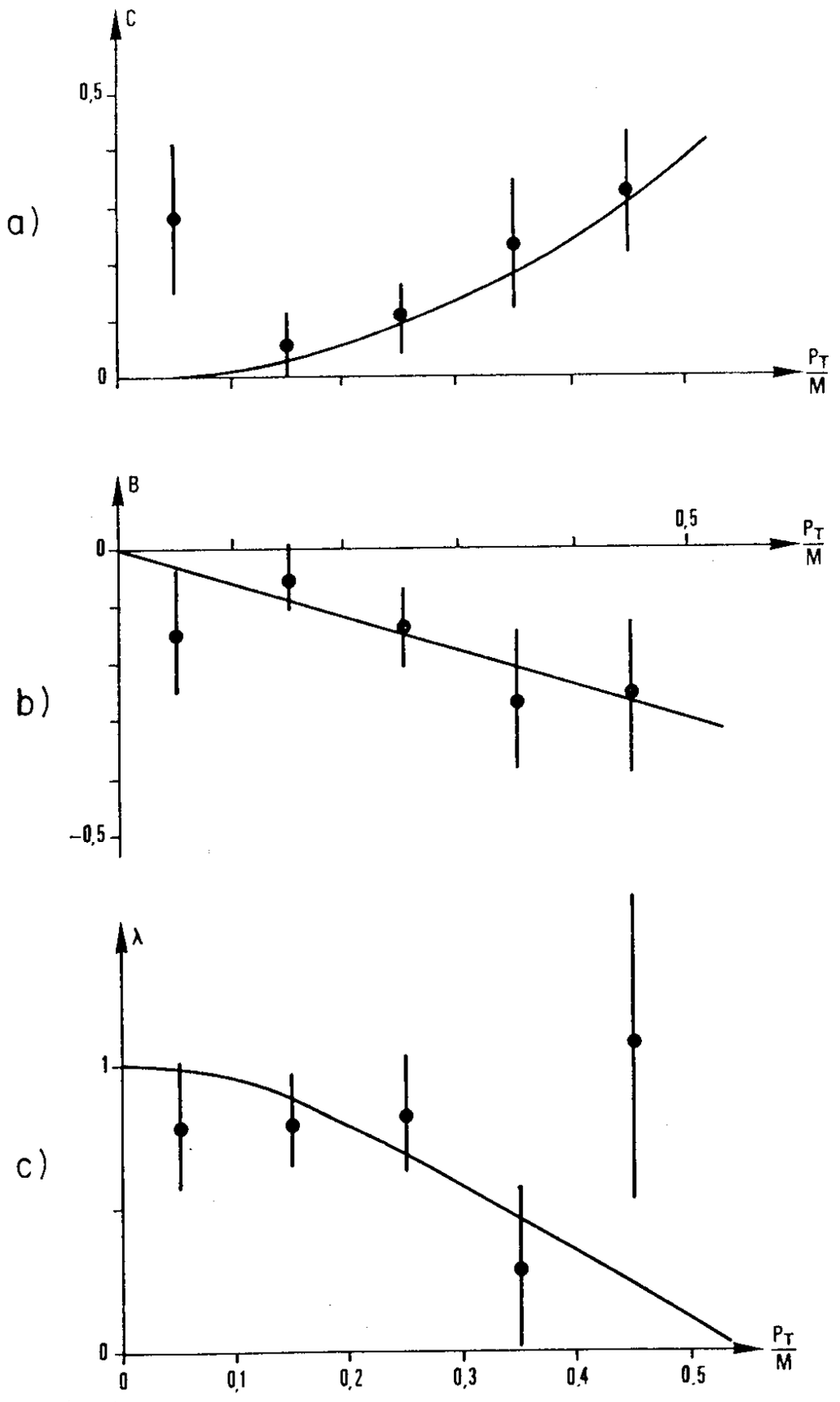

FIG. 3

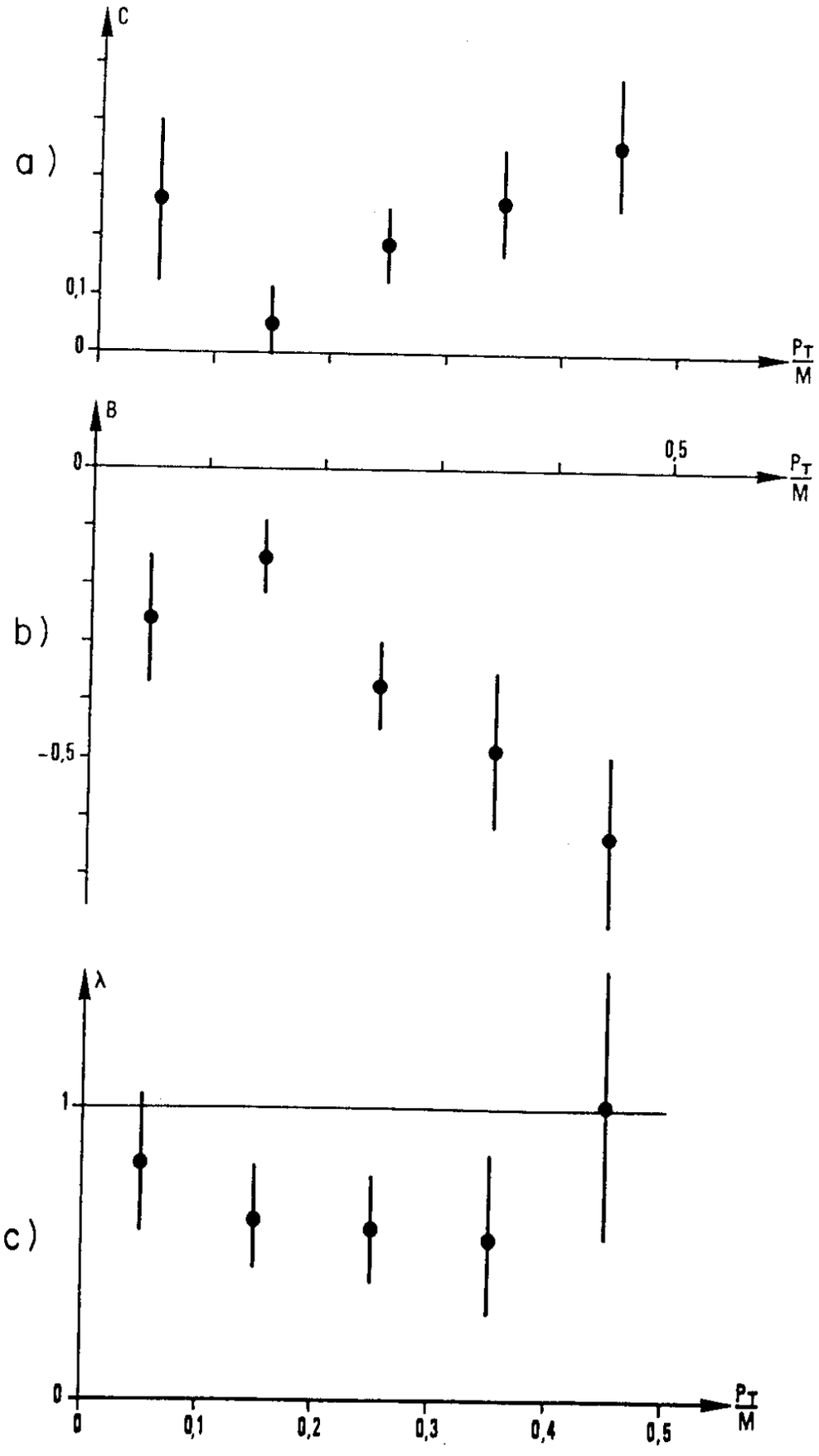

FIG. 4

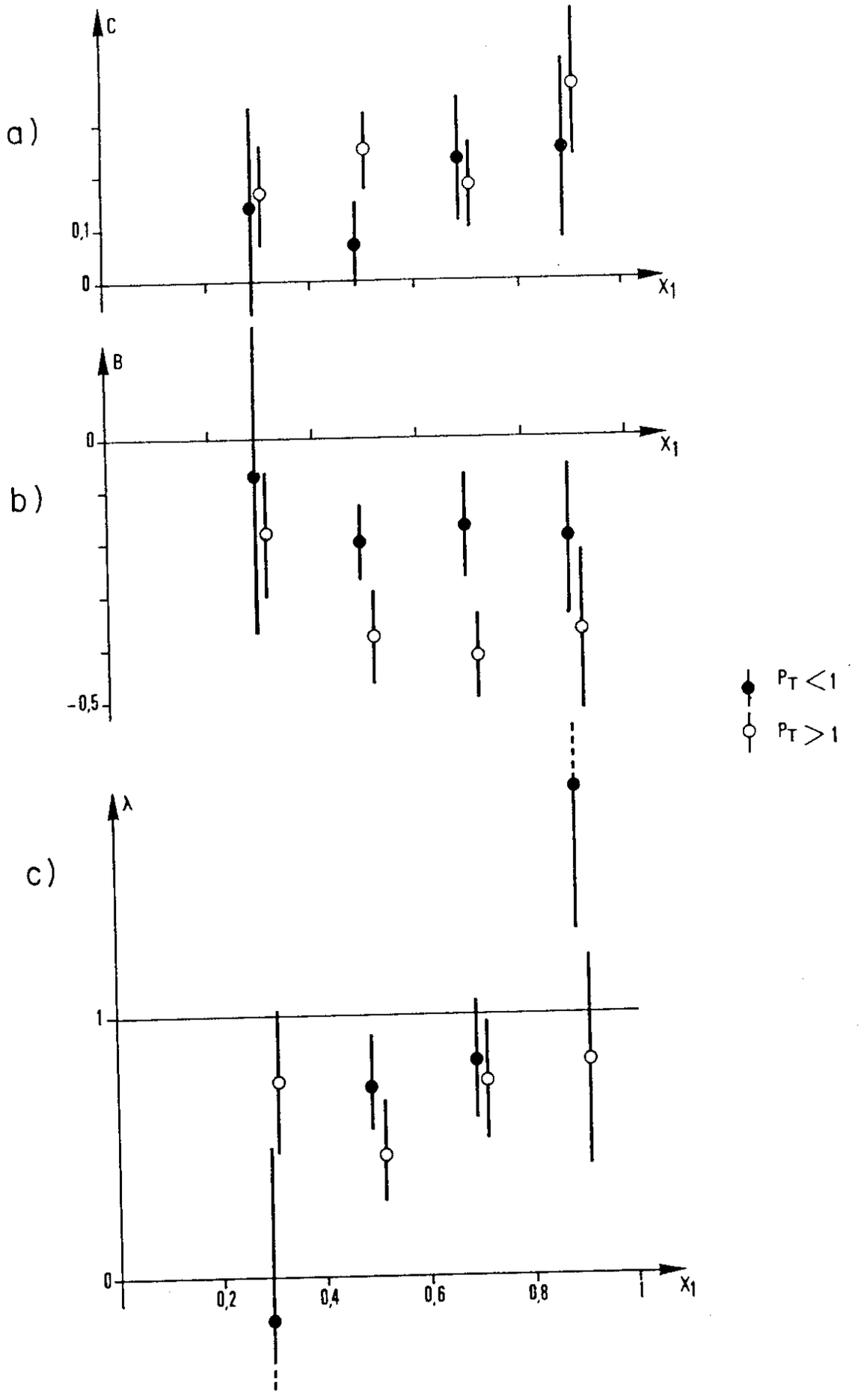

FIG. 5

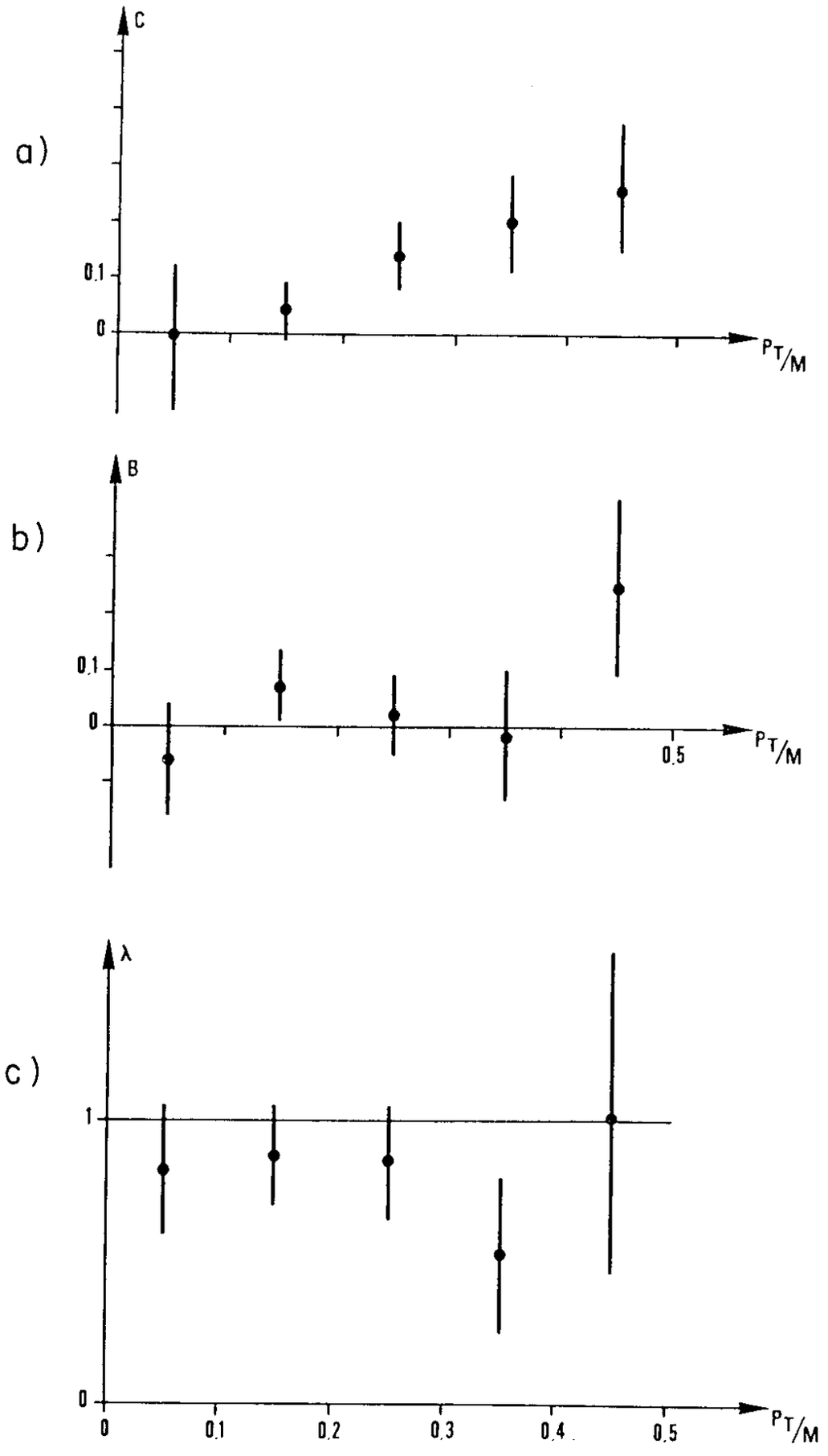

FIG . 6

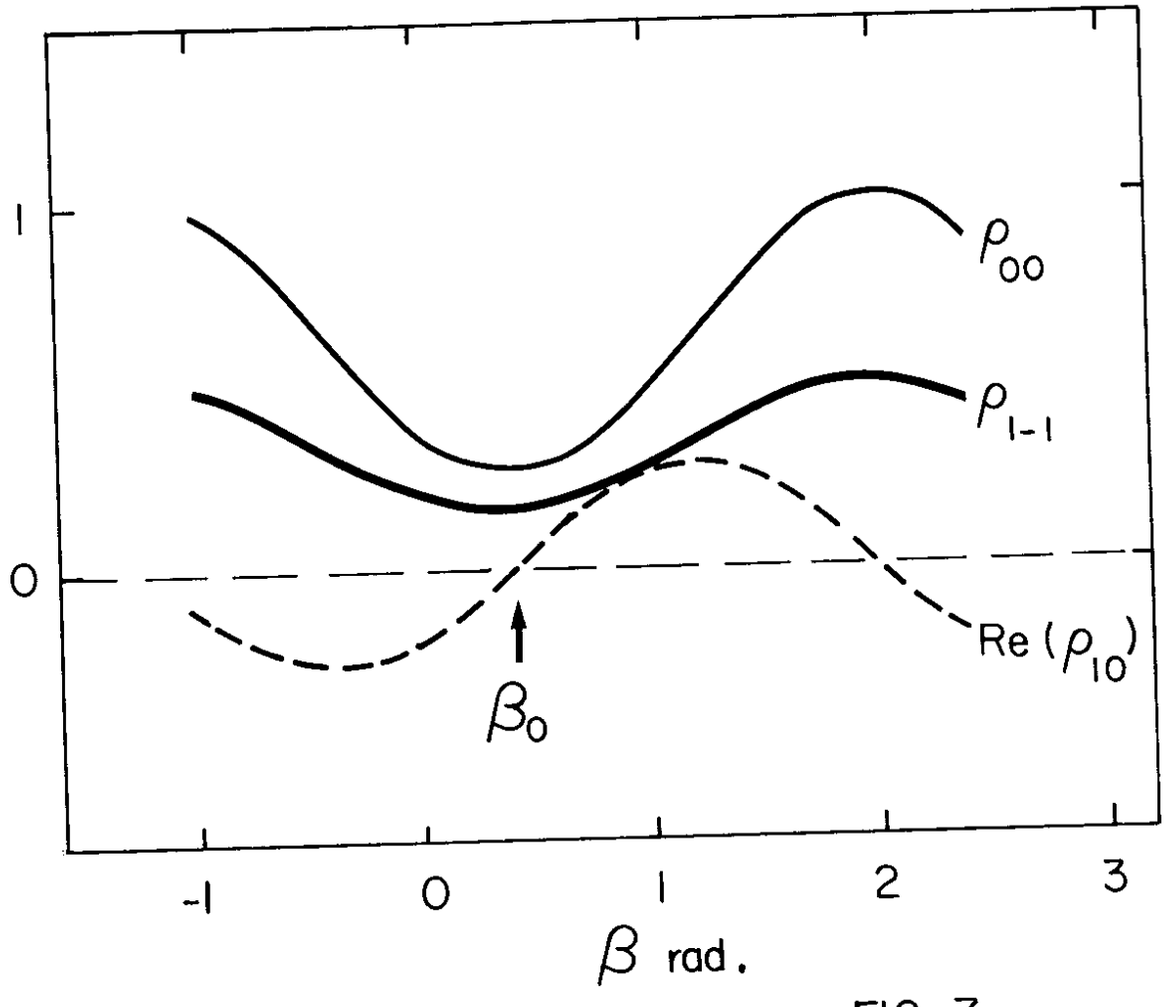

FIG. 7

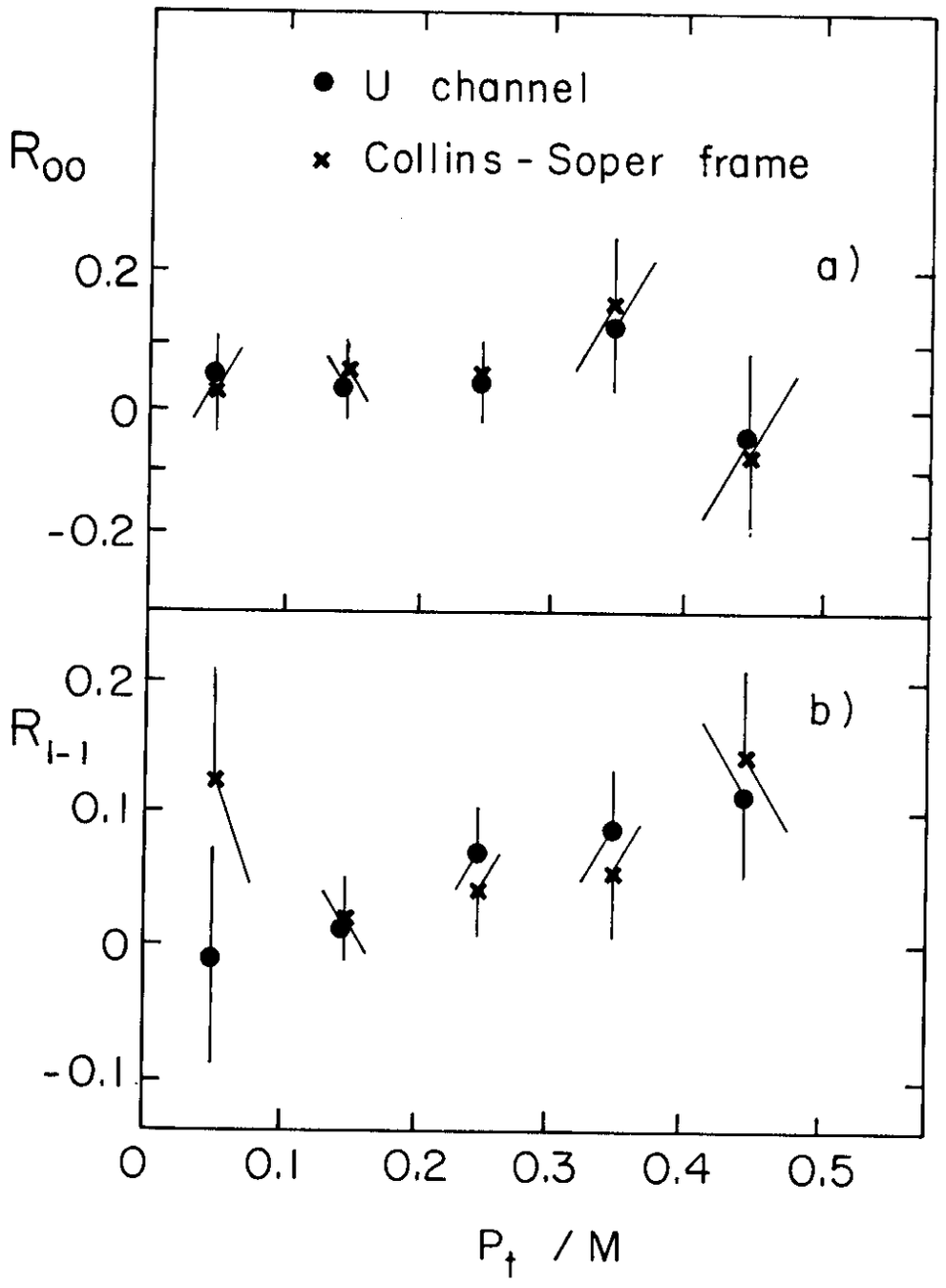
● U channel
× Collins - Soper frame
R_{oo}
a)
0.2
0
-0.2
R_{1-1}
b)
0.2
0.1
0
-0.1
0
0.1
0.2
0.3
0.4
0.5
P_t / M

FIG.8

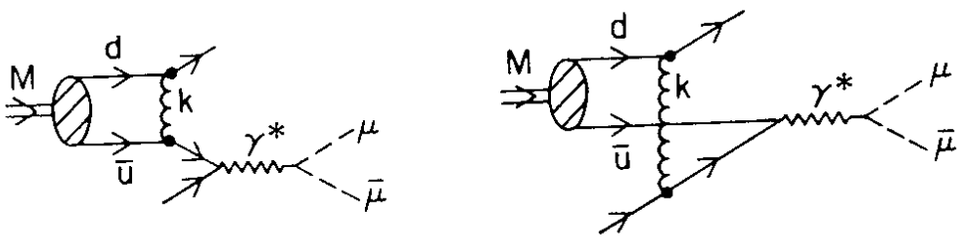

FIG. 9